



Published in final edited form as:

Angew Chem Int Ed Engl. 2017 August 21; 56(35): 10433–10437. doi:10.1002/anie.201705014.

Heterogeneous Microtesla SABRE Enhancement of ^{15}N NMR Signals

Dr. Kirill V. Kovtunov^{[a],[b]}, Dr. Larisa M. Kovtunova^{[c],[b]}, Max E. Gemeinhardt^[d], Dr. Andrey V. Bukhtiyarov^[c], Jonathan Gesiorski^[d], Prof. Valerii I. Bukhtiyarov^[c], Prof. Eduard Y. Chekmenev^[f], Prof. Igor V. Koptuyug^{[a],[b]}, and Prof. Boyd M. Goodson^{[d],[e]}

^[a]Laboratory of Magnetic Resonance Microimaging, International Tomography Center, SB RAS, 3A Institutskaya St., Novosibirsk 630090 (Russia)

^[b]Novosibirsk State University, 2 Pirogova St., Novosibirsk 630090 (Russia)

^[c]Boreskov Institute of Catalysis SB RAS, 5 Acad. Lavrentiev Pr., Novosibirsk 630090 (Russia)

^[d]Department of Chemistry and Biochemistry, Southern Illinois University, Carbondale, IL 62901 (United States)

^[e]Materials Technology Center, Southern Illinois University, Carbondale, IL 62901 (United States)

^[f]Vanderbilt University Institute of Imaging Science (VUIIS), Department of Radiology, Department of Biomedical Engineering, Department of Physics and Astronomy, VICC, Nashville, Tennessee, 37232-2310 (United States), Russian Academy of Sciences, Leninskiy Prospekt 14, 119991 Moscow (Russia)

Abstract

The hyperpolarization of heteronuclei via Signal Amplification by Reversible Exchange (SABRE) was investigated under conditions of heterogeneous catalysis and microtesla magnetic fields. Immobilization of $[\text{IrCl}(\text{COD})(\text{IMes})]$, [IMes = 1,3-bis(2,4,6-trimethylphenyl)imidazole-2-ylidene; COD = cyclooctadiene] catalyst onto silica particles modified with $\text{NH}_2(\text{CH}_2)_3$ -linkers engenders an effective heterogeneous SABRE (HET-SABRE) catalyst that was used to demonstrate $\sim 10^2$ -fold enhancement of ^{15}N NMR signals in pyridine at 9.4 T following parahydrogen bubbling within a magnetic shield. No ^{15}N NMR enhancement was observed from the supernatant liquid following catalyst separation, which along with XPS characterization, supports that the effects result from SABRE under heterogeneous catalytic conditions. The technique can be developed further for producing catalyst-free agents via SABRE with hyperpolarized heteronuclear spins, and thus is promising for biomedical NMR and MRI applications.

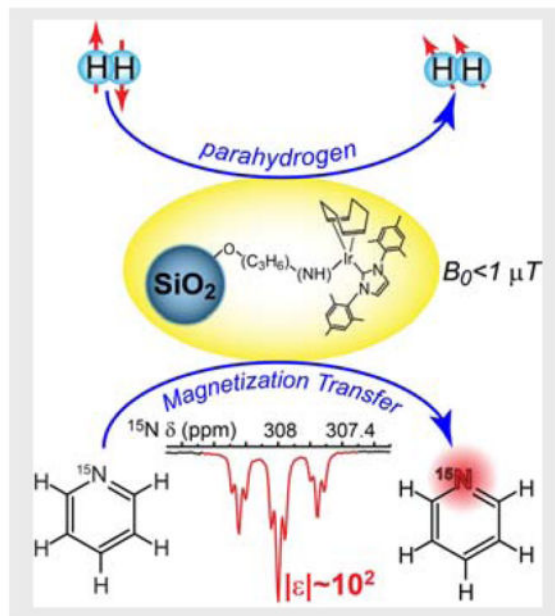
Making the insensitive, sensitive

A novel heterogeneous catalyst for NMR enhancement was prepared by immobilizing an iridium-based catalyst on silica microparticles. Addition of parahydrogen--a source of nuclear spin order--

Correspondence to: Kirill V. Kovtunov; Boyd M. Goodson.

Supporting Information for this article is given via a link at the end of the document.

within a magnetic shield led to enhancement of ^{15}N NMR signals by ~ 100 -fold. The catalyst particles are easy to separate, which should allow substrates with hyper-polarized heteronuclei to be prepared free of contamination by the catalyst.



Keywords

parahydrogen; heterogeneous catalyst; HET-SABRE; hyperpolarization; heteronuclei

A variety of different methods have been developed over the years to achieve NMR signal enhancement via hyperpolarization—the generation of highly non-equilibrium nuclear spin polarization—thereby overcoming the sensitivity problems of standard NMR/MRI techniques.^[1–4] One such technique is dissolution dynamic nuclear polarization (d-DNP),^[5] which allows different (e.g.) ^{13}C - and ^{15}N -containing molecules to be hyperpolarized and used in biomedical investigations.^[6–10] Alternatively, methods involving parahydrogen-induced polarization (PHIP)^[11,12] and Signal Amplification by Reversible Exchange (SABRE)^[13,14] have demonstrated the ability to provide significant polarization enhancements using simple, highly economical setups; moreover, these parahydrogen-based methods are of interest because they are rapid (acting in seconds or 10s of seconds) and potentially can have high agent throughput with continuous agent generation.

In parahydrogen-based methods an organometallic catalyst is used to form a coordination complex between the parahydrogen (*para*- H_2) and the target substrate molecule^[1]: In “traditional” PHIP, this allows hydrogenation of unsaturated bonds and hence a transfer of spin order to the substrate; however in SABRE, spin order is transferred spontaneously through the *J*-coupling network without requiring permanent chemical change to the substrate.

Although great progress has been achieved over a relatively short period of time,^[15–21] a limitation that continues to exist for both PHIP and SABRE is the presence of the organometallic catalyst in the solution after substrate polarization has been achieved, hindering a number of potential biological and biomedical applications that would be affected by such contamination. In addition, catalyst recovery would be highly desirable to permit later re-use. As such there has been interest in developing approaches that use heterogeneous catalysts (i.e. where the catalyst is in a different phase from the substrate) to combat these issues and better enable implementation of parahydrogen-based approaches for medical/imaging applications. Recent work towards that end includes the immobilization of homogeneous complexes to solid supports for SABRE^[22,23] and for PHIP^[17,24,25] or supported/bulk metal/metal oxide catalysts use for PHIP.^[17,26–29]

The nature of the hyperpolarized substrates is also important. For example, because of the long spin-lattice relaxation times (T_1 's) of many heteronuclei, hyperpolarization of heteronuclear spins can significantly extend the lifetime of the resulting non-equilibrium polarization compared to that of polarized protons.^[30,31] Indeed, recent demonstrations of hyperpolarization of important nuclei (with reduced detection sensitivity compared to ^1H , but often greater spectral sensitivity in addition to much longer T_1 values) as ^{15}N ,^[32–35] ^{13}C ,^[1,36–38] ^{31}P ,^[39–41] and even ^{119}Sn and ^{29}Si ^[42] are reported for both homogeneous SABRE^[43] and homogeneous PHIP^[44]; however, to date the transfer of polarization to heteronuclei under heterogeneous catalytic conditions (wherein the substrate is in a different phase than the catalyst) was reported only for the PHIP technique.^[31,45,46] Nevertheless, the intrinsic advantages of the SABRE approach^[13] would make the production of heteronuclear hyperpolarization via SABRE under heterogeneous catalytic conditions (i.e. HET-SABRE)^[22,23] highly desirable.

Toward that end, here we combine heterogeneous SABRE with the ability to polarize ^{15}N nuclei. A signal enhancement of ~100-fold was reached for the ^{15}N resonance of ^{15}N -pyridine molecules using a novel hetero-geneous SABRE catalyst $(\text{SiO}_2)_x\text{-(C}_3\text{H}_6\text{)-NH}$ Ir(COD)(IMes), where IMes = 1,3-bis(2,4,6-trimethylphenyl)imidazole-2-ylidene, COD = cyclooctadiene.

The preparation of the HET-SABRE catalyst used in the present work is briefly summarized below: First, the homogeneous SABRE catalyst $[\text{Ir}(\text{COD})(\text{IMes})\text{Cl}]$ ^[47] was synthesized as previously reported.^[18,47–49] Then 90 mg of this $[\text{Ir}(\text{COD})(\text{IMes})\text{Cl}]$ powder and 400 mg of 3-aminopropyl-functionalized silica gel (~40–63 μm ; Millipore-Sigma 364258) were added in a Schlenk tube and dried under vacuum for 30 min. After back-filling with argon gas, 10 ml of dried and deoxygenated benzene was transferred to the Schlenk tube via syringe and the reaction mixture was stirred for 24 h. Three drops of triethylamine (Millipore-Sigma 121-44-8) were then added to the reaction mixture with stirring continued for an additional 6 h. The solid material was filtered and washed with benzene until the supernatant solution was colorless; the catalyst particles were then washed with methanol several times and dried under vacuum for 2 h to give the pre-activated heterogeneous SABRE (HET-SABRE) catalyst (Fig. 1).

In order to test its viability to perform HET-SABRE, the catalyst was first investigated to see if it could be used to enhance ^1H NMR signals of pyridine. To this end, 10 mg of the HET-SABRE catalyst was placed inside a 5 mm NMR tube along with 15 μL of pyridine dissolved in 0.5 ml of CD_3OD . Parahydrogen gas (75 psi, enriched to 50% *para*- H_2 isomer) was then bubbled into the reaction mixture via Teflon capillary tubing, which extended to the bottom of the NMR tube. After 10 s of *para*- H_2 bubbling within the fringe field of the NMR spectrometer (\sim tens of Gauss), the sample was quickly transferred to the high field (9.4 T) of an NMR spectrometer and enhanced ^1H signals were detected from the free py substrate (Figure S3). Although the observed ^1H polarization enhancement (\sim 2.6-fold) was smaller than that achieved in previous HET-SABRE efforts,^[22,23] the point of this initial experiment was merely to qualitatively validate the catalyst for later studies of heteronuclear polarization enhancement, and no attempt was made to improve the enhancement by optimizing experimental parameters (*e.g.* *para*- H_2 fraction, SABRE mixing field, temperature, concentrations, etc.). Nevertheless, in order to ensure the heterogeneous nature of the observed ^1H polarization enhancement, the HET-SABRE catalyst particles were filtered out and the experiment was repeated with the supernatant solution; no detectable ^1H polarization enhancement was observed.

Observation of HET-SABRE enhancement of ^1H NMR signals enabled the catalyst to be tested for efficacy in generating heteronuclear (here, ^{15}N) polarization under heterogeneous catalytic conditions. Figure 2 shows successful enhancement of ^{15}N NMR signals from ^{15}N -labeled py (^{15}N -py) achieved via the so-called “SABRE-SHEATH”^[30,32] (Signal Amplification by Reversible Exchange in SHield Enables Alignment Transfer to Heteronuclei) approach. Here, 10 mg of the HET-SABRE catalyst was added to a (protonated) methanol solution containing 100 mM ^{15}N -py; the solvent was changed to MeOH because of mild concern that the quadrupolar ^2H nuclei in solvent molecules, which may transiently enter the inner sphere of the complex,^[50,51] could reduce polarization efficiency inside the magnetic shield.^[52–54] A strong polarized ^{15}N resonance was observed following 30 s bubbling of 50% *para*- H_2 inside a magnetic shield and rapid transfer to 9.4 T for detection (Fig. 2d). Spectra resolution was sufficient to resolve the expected fine structure of the ^{15}N spectrum from scalar couplings with neighboring ^1H spins (Fig. 2d *inset*). A corresponding thermally polarized ^{15}N spectrum from the sample is shown in Fig. 2b, indicating a \sim 100-fold enhancement for the hyperpolarized signals in Fig. 2d. This enhancement value is \sim 2.5 times higher than the best previously reported numbers for ^1H HET-SABRE,^[23] although the better comparison is to the \sim 5-fold enhancement values in Ref. 22, where the catalyst support particles were closer in size to those used here (indicating a larger enhancement than what would be explained simply by the \sim 10-fold decrease in gyromagnetic ratio for ^{15}N compared to ^1H).

To verify the heterogeneous nature of the observed ^{15}N signal enhancement in Fig. 2d, the HET-SABRE catalyst was removed by filtration and *para*- H_2 was bubbled through the supernatant liquid under the same experimental conditions (including use of the magnetic shield). The resulting spectrum is shown in Fig. 2c, and exhibits no discernible SABRE enhancement of the ^{15}N signal. This lack of ^{15}N SABRE-SHEATH signal with the supernatant solution (in the absence of HET-SABRE catalyst particles) supports the

conclusion that the observed ^{15}N enhancements are the result of HET-SABRE, and not homogeneous SABRE from leached catalyst moieties.

Additional supportive evidence comes from comparing the ^{15}N NMR spectrum obtained with the present heterogeneous catalyst with a corresponding spectrum obtained using homogeneous catalysts (Fig. 3). Whereas both ^{15}N NMR spectra show clear hyperpolarized ^{15}N resonances assigned to free ^{15}N -py substrate, only the solution containing the homogeneous catalysts exhibits additional peaks in the 240–270 ppm range—peaks that are attributed to equatorially and axially bound py, respectively.^[30] If the enhanced signal in Figures 2d/3a were obtained from leached homogeneous catalyst moieties, then one would expect to see corresponding peaks from catalyst-bound substrate; however, the peaks from substrate bound to the heterogeneous catalyst particles are too weak (and/or too broadened) to manifest significantly in the observed spectra (consistent with previous ^1H results with microscale HET-SABRE particles).^[22] While $\epsilon_{^{15}\text{N}} \sim 100$ fold is ~ 10 times lower than that using homogeneous variant of this catalyst (when taking into account *para*- H_2 enrichment),^[32] no temperature or field optimization was performed here. Indeed, when the homogeneous catalyst was used for these experiments (Fig. 3b), it showed ~ 4 times better SABRE polarization performance with 50 mM ^{15}N -py. We anticipate that future optimization of temperature, SABRE-SHEATH field, catalyst to substrate ratio, *para*- H_2 pressure, flow rate, etc. will allow for significant improvement of the performance of this catalyst material.^[33,53]

Finally, the HET-SABRE catalyst was also studied via XPS and ICP-MS (inductively coupled plasma mass spectrometry—see SI). Via XPS it was shown (Figure S1) that the amount of iridium is the same before and after catalyst use in the SABRE-SHEATH experiments. Similarly, levels of Ir measured by ICP-MS were similar for a supernatant solution (collected after H_2 bubbling and subsequent catalyst filtration) and a reference solution of MeOH and pyridine (Figure S3). These results thus provide additional support for the strong immobilization of the active (originally homogeneous) catalyst at the surfaces of the modified silica particles and a lack of leaching of the catalyst moieties into the solution—and hence, the conclusion that the enhancement in Fig. 2b is truly the result of a heterogeneous catalytic process.

In conclusion, the enhancement of heteronuclear (^{15}N) NMR signals via SABRE-SHEATH under heterogeneous catalytic conditions is reported for the first time. A ^{15}N polarization enhancement of ~ 100 -fold is demonstrated with 50% *para*- H_2 fraction using a novel HET-SABRE catalyst preparation, and NMR and XPS results are consistent with the conclusion that the enhancements are the result of the HET-SABRE effect—and not the result of homogeneous SABRE from any leached catalyst species. Given the fact that a variety of experimental conditions were not optimized (e.g. support particle size and catalyst surface loading, in addition to those parameters listed farther above), and the fact that enhancements of the same order were observed for the homogeneous catalyst under the same conditions, much larger ^{15}N enhancements are anticipated to result from ongoing work. The catalyst described here also has the potential for future modifications to render its hyperpolarization in aqueous media,^[55–57] which is highly synergistic with recent demonstrations of ^{15}N SABRE-SHEATH in an aqueous medium^[58] and would ultimately pave the way to

production of pure (from catalyst) ^{15}N hyperpolarized biomolecules in aqueous media for biomedical use. Indeed, our efforts will be directed not only toward improving enhancements via such experimental optimization, but also preparation of biologically relevant agents (including the targeting of other nuclei), as well as agent separation and use (and catalyst re-use) for various biological/biomedical applications.

Supplementary Material

Refer to Web version on PubMed Central for supplementary material.

Acknowledgments

We thank NSF (CHE-1416432 & CHE-1416268) NIH (1R21EB018014 & 1R21EB020323), and DoD (CDMRP BRP W81XWH-12-1-0159/BC112431, & PRMRP W81XWH-15-1-0271 & W81XWH-15-1-0272). IVK and KVK thank RFBR (16-03-00407-a and 17-54-33037) and FASO Russia project # 0333-2016-0001 for basic funding. KVK acknowledges the MK-4498.2016.3 grant. EYC & BMG respectively acknowledge the Exxon Mobil Knowledge Build & SIUC MTC. The BIC team thanks Russian Science Foundation (grant #14-23-00146) for supporting catalyst characterization.

References

1. Green RA, Adams RW, Duckett SB, Mewis RE, Williamson DC, Green GGR. *Prog Nucl Magn Reson Spectrosc.* 2012; 67:1–48. [PubMed: 23101588]
2. Barskiy DA, Coffey AM, Nikolaou P, Mikhaylov DM, Goodson BM, Branca RT, Lu GJ, Shapiro MG, Telkki V, Zhivonitko VV, et al. *Chem Eur J.* 2017; 23:725–751. [PubMed: 27711999]
3. Nikolaou P, Goodson BM, Chekmenev EY. *Chem Eur J.* 2015; 21:3156–3166. [PubMed: 25470566]
4. Comment A, Merritt ME. *Biochemistry.* 2014; 53:7333–7357. [PubMed: 25369537]
5. Ardenkjaer-Larsen JH, Fridlund B, Gram A, Hansson G, Hansson L, Lerche MH, Servin R, Thaning M, Golman K. *Proc Natl Acad Sci U S A.* 2003; 100:10158–63. [PubMed: 12930897]
6. Milani J, Vuichoud B, Bornet A, Melzi R, Jannin S, Bodenhausen G. *Rev Sci Instrum.* 2017; 88:15109.
7. Nelson SJ, Kurhanewicz J, Vigneron DB, Larson PEZ, Harzstark AL, Ferrone M, Van Criekinge M, Chang JW, Park I, Reed G, et al. *Sci Transl Med.* 2013; 5:198ra108.
8. Durst M, Chiavazza E, Haase A, Aime S, Schwaiger M, Schulte RF. *Magn Reson Med.* 2016; 76:1900–1904. [PubMed: 26822562]
9. Kurhanewicz J, Vigneron DB, Brindle K, Chekmenev EY, Comment A, Cunningham CH, Deberardinis RJ, Green GG, Leach MO, Rajan SS, et al. *Neoplasia.* 2011; 13:81–97. [PubMed: 21403835]
10. Cudalbu C, Comment A, Kurdzesau F, Heeswijk RB, Uffmann K, Jannin S, Denisov V, Kirike D, Gruetter R. *Phys Chem Chem Phys.* 2010; 12:5818–5823. [PubMed: 20461252]
11. Bowers CR, Weitekamp DP. *J Am Chem Soc.* 1987; 109:5541–5542.
12. Pravica MG, Weitekamp DP. *Chem Phys Lett.* 1988; 145:255–258.
13. Adams RW, Aguilar JA, Atkinson KD, Cowley MJ, Elliott PIP, Duckett SB, Green GGR, Khazal IG, López-Serrano J, Williamson DC. *Science.* 2009; 323:1708–1711. [PubMed: 19325111]
14. Adams RW, Duckett SB, Green RA, Williamson DC, Green GGR. *J Chem Phys.* 2009; 131:194505. [PubMed: 19929058]
15. Duckett SB, Wood NJ. *Coord Chem Rev.* 2008; 252:2278–2291.
16. Hövener JB, Schwaderlapp N, Borowiak R, Lickert T, Duckett SB, Mewis RE, Adams RW, Burns MJ, Highton LAR, Green GGR, et al. *Anal Chem.* 2014; 86:1767–1774. [PubMed: 24397559]
17. Kovtunov KV, Zhivonitko VV, Skovpin IV, Barskiy DA, Koptyug IV. *Top Curr Chem.* 2013; 338:123–180. [PubMed: 23097028]

18. Barskiy DA, Kovtunov KV, Koptyug IV, He P, Groome KA, Best QA, Shi F, Goodson BM, Shchepin RV, Coffey AM, et al. *J Am Chem Soc.* 2014; 136:3322–3325. [PubMed: 24528143]
19. Zhou R, Zhao EW, Cheng W, Neal LM, Zheng H, Quiñones RE, Hagelin-Weaver HE, Bowers CR. *J Am Chem Soc.* 2015; 137:1938–1946. [PubMed: 25629434]
20. Salnikov OG, Kovtunov KV, Koptyug IV. *Sci Rep.* 2015; 5:13930. [PubMed: 26349543]
21. Kovtunov KV, Barskiy DA, Coffey AM, Truong ML, Salnikov OG, Khudorozhkov AK, Inozemtseva EA, Prosvirin IP, Bukhtiyarov VI, Waddell KW, et al. *Chem - A Eur J.* 2014; 20:11636–11639.
22. Shi F, Coffey AM, Waddell KW, Chekmenev EY, Goodson BM. *Angew Chemie - Int Ed.* 2014; 53:7495–7498.
23. Shi F, Coffey AM, Waddell KW, Chekmenev EY, Goodson BM. *J Phys Chem C.* 2015; 119:7525–7533.
24. Koptyug IV, Kovtunov KV, Burt SR, Anwar MS, Hilty C, Han SI, Pines A, Sagdeev RZ. *J Am Chem Soc.* 2007; 129:5580–5586. [PubMed: 17408268]
25. Abdhussain S, Breitzke H, Ratajczyk T, Grünberg A, Srour M, Arnaut D, Weidler H, Kunz U, Kleebe HJ, Bommerich U, et al. *Chem Eur J.* 2014; 20:1159–1166. [PubMed: 24338904]
26. Kovtunov KV, Beck IE, Bukhtiyarov VI, Koptyug IV. *Angew Chemie - Int Ed.* 2008; 47:1492–1495.
27. Zhao EW, Zheng H, Zhou R, Hagelin-Weaver HE, Bowers CR. *Angew Chemie - Int Ed.* 2015; 54:14270–14275.
28. Glogler S, Grunfeld AM, Ertas YN, McCormick J, Wagner S, Schleker PPM, Bouchard LS. *Angew Chemie - Int Ed.* 2015; 54:2452–2456.
29. Burueva DB, Romanov AS, Salnikov OG, Zhivonitko VV, Chen YW, Barskiy DA, Chekmenev EY, Hwang DWH, Kovtunov KV, Koptyug IV. *J Phys Chem C.* 2017; 121:4481–4487.
30. Truong ML, Theis T, Coffey AM, Shchepin RV, Waddell KW, Shi F, Goodson BM, Warren WS, Chekmenev EY. *J Phys Chem C.* 2015; 119:8786–8797.
31. Kovtunov KV, Barskiy DA, Shchepin RV, Salnikov OG, Prosvirin IP, Bukhtiyarov AV, Kovtunova LM, Bukhtiyarov VI, Koptyug IV, Chekmenev EY. *Chem Eur J.* 2016; 22:16446–16449. [PubMed: 27607402]
32. Theis T, Truong ML, Coffey AM, Shchepin RV, Waddell KW, Shi F, Goodson BM, Warren WS, Chekmenev EY. *J Am Chem Soc.* 2015; 137:1404–1407. [PubMed: 25583142]
33. Barskiy DA, Shchepin RV, Coffey AM, Theis T, Warren WS, Goodson BM, Chekmenev EY. *J Am Chem Soc.* 2016; 138:8080–8083. [PubMed: 27321159]
34. Nonaka H, Hirano M, Imakura Y, Takakusagi Y, Ichikawa K, Sando S. *Sci Rep.* 2017; 7:40104. [PubMed: 28067292]
35. Reineri F, Viale A, Ellena S, Alberti D, Boi T, Giovenzana GB, Gobetto R, Premkumar SSD, Aime S. *J Am Chem Soc.* 2012; 134:11146–11152. [PubMed: 22663300]
36. Pravdivtsev AN, Yurkovskaya AV, Zimmermann H, Vieth H, Ivanov KL. *RSC Adv.* 2015; 5:63615–63623.
37. Golman K, Axelsson O, Jóhannesson H, Månsson S, Olofsson C, Petersson JS. *Magn Reson Med.* 2001; 46:1–5. [PubMed: 11443703]
38. Coffey AM, Shchepin RV, Truong ML, Wilkens K, Pham W, Chekmenev EY. *Anal Chem.* 2016; 88:8279–8288. [PubMed: 27478927]
39. Zhivonitko VV, Skovpin IV, Koptyug IV. *Chem Commun.* 2015; 51:2506–2509.
40. Burns MJ, Rayner PJ, Green GGR, Highton LAR, Mewis RE, Duckett SB. *J Phys Chem B.* 2015; 119:5020–5027. [PubMed: 25811635]
41. Jóhannesson H, Axelsson O, Karlsson M. *Comptes Rendus Phys.* 2004; 5:315–324.
42. Olaru AM, Burt A, Rayner PJ, Hart SJ, Whitwood AC, Green GGR, Duckett SB. *Chem Commun.* 2016; 52:14482–14485.
43. Mewis RE. *Magn Reson Chem.* 2015; 53:789–800. [PubMed: 26264565]
44. Kuhn LT, Bargon J. *Top Curr Chem.* 2007; 276:25–68.

45. Kovtunov KV, Barskiy DA, Salnikov OG, Shchepin RV, Coffey AM, Kovtunova LM, Bukhtiyarov VI, Koptyug IV, Chekmenev EY. *RSC Adv.* 2016; 6:69728–69732. [PubMed: 28042472]
46. Glöggl S, Grunfeld AM, Ertas YN, McCormick J, Wagner S, Schleker PPM, Bouchard LS. *Angew Chemie - Int Ed.* 2015; 54:2452–2456.
47. Cowley MJ, Adams RW, Atkinson KD, Cockett MCR, Duckett SB, Green GGR, Lohman JaB, Kerssebaum R, Kilgour D, Mewis RE. *J Am Chem Soc.* 2011; 133:6134–6137. [PubMed: 21469642]
48. Barskiy DA, Kovtunov KV, Koptyug IV, He P, Groome KA, Best QA, Shi F, Goodson BM, Shchepin RV, Truong ML, et al. *ChemPhysChem.* 2014; 15:4100–4107. [PubMed: 25367202]
49. Vazquez-serrano LD, Owens BT, Buriak JM. 2006; 359:2786–2797.
50. Moreno KX, Nasr K, Milne M, Sherry AD, Goux WJ. *J Magn Reson.* 2015; 257:15–23. [PubMed: 26037136]
51. Van Weerdenburg BJA, Engwerda AHJ, Eshuis N, Longo A, Banerjee D, Tessari M, Guerra F, Rutjes PJT, Bickelhaupt FM, Feiters MC. *Chem Eur J.* 2015; 21:10482–10489. [PubMed: 26072737]
52. Shchepin RV, Barskiy DA, Mikhaylov DM, Chekmenev EY. *Bioconj Chem.* 2016; 27:878–882.
53. Shchepin RV, Truong ML, Theis T, Coffey AM, Shi F, Waddell KW, Warren WS, Goodson BM, Chekmenev EY. *J Phys Chem Lett.* 2015; 6:1961–1967. [PubMed: 26029349]
54. Barskiy DA, Shchepin RV, Tanner CPN, Colell JFP, Goodson BM, Theis T, Warren WS, Chekmenev EY. *ChemPhysChem.* 2017; 18:1493–1498. [PubMed: 28517362]
55. Truong ML, Shi F, He P, Yuan B, Plunkett KN, Coffey AM, Shchepin RV, Barskiy DA, Kovtunov KV, Koptyug IV, et al. *J Phys Chem B.* 2014; 118:13882–13889. [PubMed: 25372972]
56. Shi F, He P, Best QA, Groome K, Truong ML, Coffey AM, Zimay G, Shchepin RV, Waddell KW, Chekmenev EY, Goodson BM. *J Phys Chem C.* 2016; 120:12149–12156.
57. Spannring P, Reile I, Emondts M, Schleker PPM, Hermkens NKJ, van der Zwaluw NGJ, van Weerdenburg BJA, Tinnemans P, Tessari M, Blümich B, et al. *Chem Eur J.* 2016; 22:9277–9282. [PubMed: 27258850]
58. Colell JFP, Emondts M, Logan AWJ, Shen K, Bae J, Shchepin RV, Ortiz GX, Spannring P, Wang Q, Malcolmson SJ, et al. *J Am Chem Soc.* 2017; 139:7761–7767. [PubMed: 28443329]

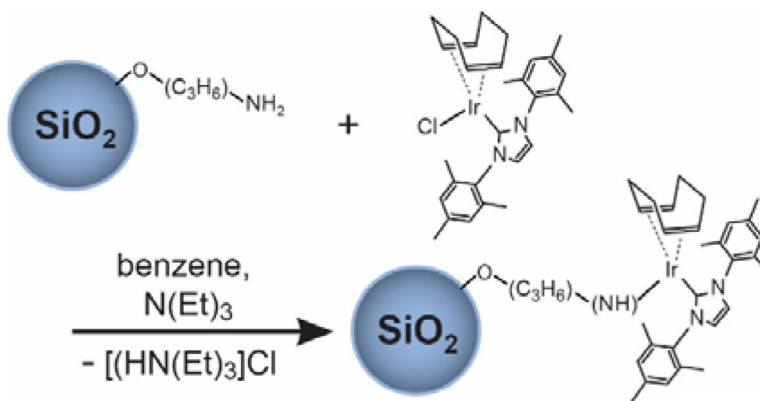


Figure 1. Scheme summarizing synthesis of the HET-SABRE catalyst via immobilization of Ir(COD)(IMes)Cl to NH₂(CH₂)₃-modified silica particles (the COD is hydrogenated during activation and dissociates from the catalyst).

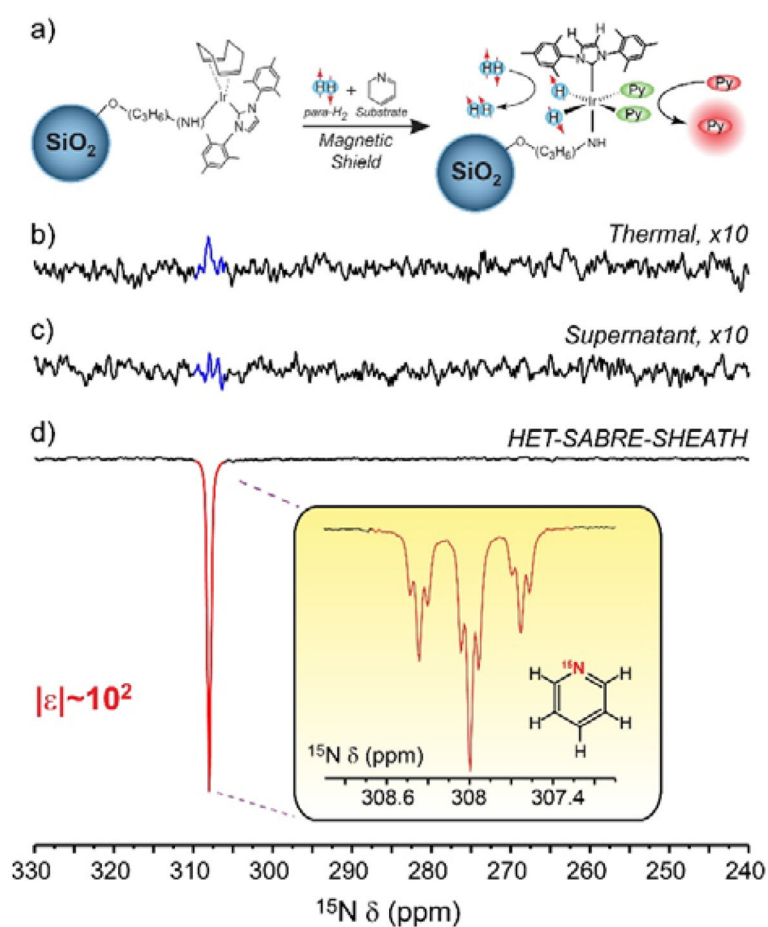


Figure 2.

(a) Scheme of the heterogeneous SABRE-SHEATH experiment. (b–d) Selected ¹⁵N spectra from “HET-SABRE-SHEATH” experiments (line broadening (l.b.): 10 Hz). (b) Thermally-polarized ¹⁵N signal from 100 mM ¹⁵N-py (10 mg catalyst/MeOH; 1 scan). (c) ¹⁵N NMR spectrum obtained from the supernatant solution recorded after HET-SABRE catalyst filtration, but otherwise conducted under the same SABRE-SHEATH experimental conditions in (d). Note the absence of enhanced ¹⁵N signal in (c); the absence of thermally polarized ¹⁵N signal similar to (b) is due to the fact that there is insufficient time for the ¹⁵N spins of the substrate to thermally equilibrate with the NMR magnet during the rapid sample transfer from the magnetic shield (¹⁵N *T*₁ > 1 min). (d) HET-SABRE-SHEATH enhancement of ¹⁵N signals from the from the ¹⁵N-py substrate, achieved prior to catalyst particle filtration used for (c); the *inset* shows the resolved ¹⁵N spectrum from free substrate (l.b.=0.2 Hz).

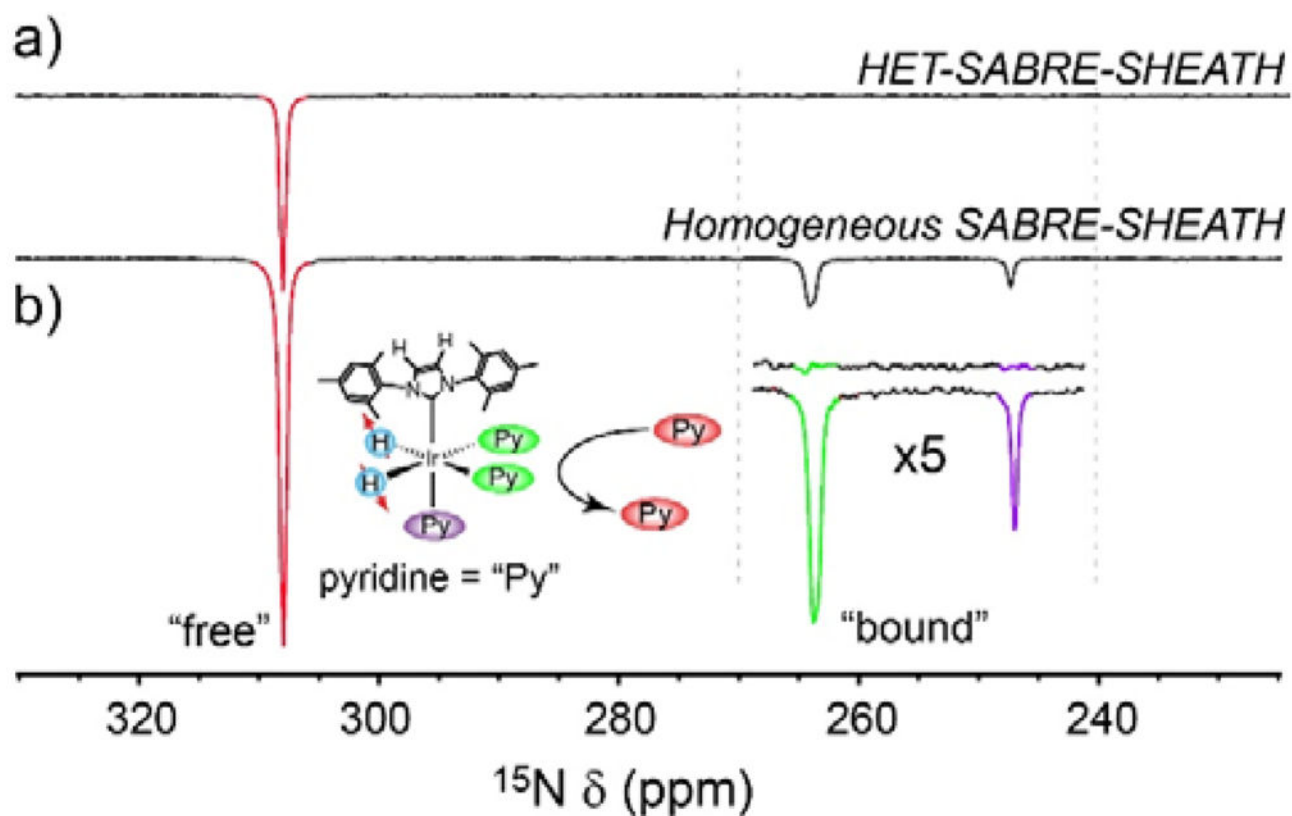


Figure 3. Comparison between the ^{15}N HET-SABRE-SHEATH result in Figure 2(a) and a corresponding ^{15}N SABRE-SHEATH spectrum obtained with the standard homogeneous catalyst (b). The ^{15}N -py concentrations were 100 mM and 50 mM, respectively and both spectra are presented in the same vertical scale. The *inset* shows the expected presence of bound substrate resonances in the spectrum obtained with the homogeneous catalyst, and the apparent absence of bound substrate peaks for the heterogeneous system.